Mechanistic Investigation of Dirhodium-Catalyzed Intramolecular Allylic C-H Amination versus Alkene Aziridination

ARTICLE *in* THE JOURNAL OF ORGANIC CHEMISTRY · SEPTEMBER 2014

Impact Factor: 4.72 · DOI: 10.1021/jo5019987 · Source: PubMed

3 AUTHORS, INCLUDING:

Xuepeng Zhang
Sun Yat-Sen University
16 PUBLICATIONS **55** CITATIONS
SEE PROFILE

Huiying Xu
Sun Yat-Sen University
12 PUBLICATIONS **144** CITATIONS
SEE PROFILE

JOC The Journal of Organic Chemistry

Article

pubs.acs.org/joc

Mechanistic Investigation of Dirhodium-Catalyzed Intramolecular Allylic C−H Amination versus Alkene Aziridination

Xuepeng Zhang, Huiying Xu, and Cunyuan Zhao*

MOE Key Laboratory of Bioinorganic and Synthetic Chemistry, School of Chemistry and Chemical Engineering, Sun Yat-Sen University, Guangzhou 510275, P. R. China

Supporting Information

ABSTRACT: The reaction mechanisms and chemoselectivity on the intramolecular allylic C−H amination versus alkene aziridination of 4-pentenylsulfamate promoted by four elaborately selected dirhodium paddlewheel complexes are investigated by a DFT approach. A predominant singlet concerted, highly asynchronous pathway and an alternative triplet stepwise pathway are obtained in either C−H amination or alkene aziridination reactions when mediated by weak electron-donating catalysts. A singlet stepwise C−H amination pathway is obtained under strongly donating catalysts. The rate-determining step in the C−H amination is the H-abstraction process. The subsequent diradical-rebound C−N formation in the triplet pathway or the combination of the allylic carbocation and the negative changed N center in the singlet pathway require an identical energy barrier. A mixed singlet−triplet pathway is preferred in either the C−H insertion or alkene aziridination in the $Rh_2(NCH_3CHO)_4$ entry that the triplet pathway is initially favorable in the rate-determining steps, and the resultant triplet intermediates would convert to a singlet reaction coordinate. The nature of C−H amination or alkene aziridination is estimated to be a stepwise process. The theoretical observations presented in the paper are consistent with the experimental results and, more importantly, provide a thorough understanding of the nature of the reaction mechanisms and the minimum-energy crossing points.

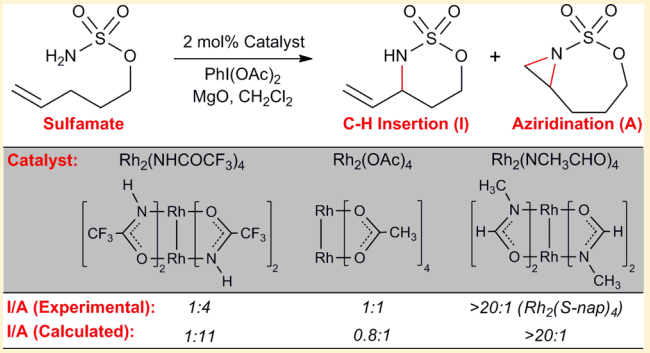

INTRODUCTION

Catalytic intramolecular C−H amination and alkene aziridination have emerged as popular synthetic protocols for the preparation of amine-derived heterocycles.[1] These methods are featured by their high efficiency, selectivity, and relative convenience. Various transition-metal complexes, particularly metal-porphyrins,[2] dirhodium paddlewheel complexes,[3] and metal Schiff base complexes[4] have been reported for their catalytic activities in these reactions. Among them, dirhodium complexes have the broadest applications, due to their structural rigidity, ease of ligand exchange, liable axial coordination sites, and proper oxidation potential.[1d]

It is generally assumed that the formation of metal-nitrene involves three major steps: (1) in situ generation of iminoiodinane PhI═NR from the substrate; (2) formation of metal-phenyliodinane $L_xM-N(IPh)R$ (intermediate 1, IM1); (3) formation of metal-nitrene (IM2) (Figure 1). The formation of substrate−oxidant complex iminoiodinane is assumed to be the overall rate-determining step, and this species reacts rapidly to give the corresponding catalyst−substrate complexes IM1 and IM2.[3m,p] Both IM1 and IM2 are assumed to be directly responsible for the nitrene delivery.[1a,2g,3p,4d,e] Che and co-workers found that the decomposition of IM1 to IM2 is a consequence of the entropy increase and the metal-nitrene (IM2) is the active species for the nitrene delivery.[5] Du Bois and co-workers also support that the reactive oxidant is metal-nitrene.[3m]

Although rate-determining steps precede the nitrene delivery events, the C−H activation/C−N formation steps are additionally important, which are considered to be product-determining. There is much debate regarding the mechanism of C−H amination. A concerted, asynchronous pathway is generally accepted,[1d,3l,m,5,6] in which a H-abstraction process occurs in the unique transition state. Physical organic experiments, such as Hammett analysis ($|\rho|$-value <1),[3j,m,p,7] KIE (kinetic isotope effect) data (<2)[3m,8] and radical-clock studies (no ring opened products)[3l,m,p,9] together support the concerted asynchronous pathway. However, Du Bois and co-workers point out that these experimental observations cannot definitively rule out a stepwise pathway.[3l] Dauban and co-workers also doubt the reliability of physical organic experiments.[10] Recently, some experimental observations and theoretical approaches suggest a stepwise pathway that the H-abstraction and C−N bond formation take place in distinct steps.[1i,3o,6h,11] The C−N bond formation step may be a barrier-free radical-rebound process[3o,5,6e−g,12] or has an identifiable energy barrier.[6h,13] Generally, a concerted C−H insertion via a singlet nitrenoid or a stepwise H-abstraction/

Received: August 29, 2014

   dx.doi.org/10.1021/jo5019987 | J. Org. Chem. XXXX, XXX, XXX−XXX

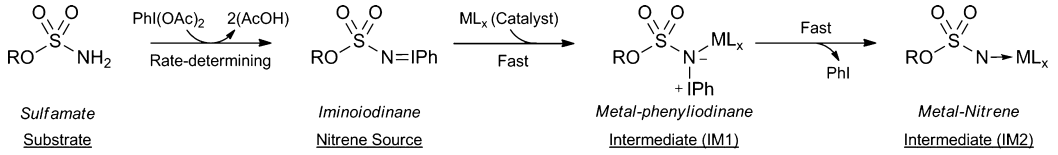

Figure 1. Shown is the proposed mechanism for the formation of metal-nitrene.

radical-recombination via a triplet nitrenoid is accepted.[3o,p,6e−h,12] It is also found that the singlet concerted C−H asymmetric insertion on a prochiral methylene center gives rise to the enantiomerically pure product with the retention of chirality, while a racemic product is obtained when the triplet stepwise pathway is predominant.[5,14]

Almost the same divergence of opinions (concerted or stepwise, singlet or triplet) on the mechanisms of alkene aziridination is under debate.[1a,d,3m,6f,15] A triplet stepwise mechanism or a singlet concerted pathway is commonly accepted. However, the results obtained from conventional physical organic experiments, such as the Hammett competition experiments and radical-clock studies, are sometimes conflicting and contradictory.[2b,16] Du Bois and co-workers speculated that the alkene aziridination involves a concerted, electrophilic oxidation process.[3m] Pérez and collaborators reported that both concerted and stepwise, singlet and triplet pathways are possible.[15] It is well accepted that the nitrene group preferentially inserts into tertiary, allylic, and benzylic C−H bonds while the chemoselectivity between the C−H amination versus alkene aziridination remains ambiguous.[3f,g,17] The predilection for alkene aziridination or C−H amination is varied with the change of catalysts.[3m] Some catalysts are strongly biased toward C−H amination,[2f,3l,o,4c,18] while a few other catalysts preferentially promote alkene aziridination.[3m,19] Dirhodium tetracarboxylate ($Rh_2(OAc)_4$), the most frequently utilized catalyst, has no predilection for either the allylic C−H amination or the alkene aziridination.[3m] The reasons for the significant chemoselectivity are not entirely apparent, despite substantial efforts that have been made in the past few decades. The aforementioned experimental methods are not sufficient enough to describe the C−H amination and alkene aziridination, and it is necessary and relatively convenient to utilize theoretical approaches to investigate the nature of these competing reactions.

Meanwhile, the distinction between concerted and stepwise pathways has not been well described so far, and other questions such as which is the predominant pathway and whether a singlet stepwise pathway exists still remain. The nature of singlet/triplet pathways and the corresponding spin crossover is also not clear yet. Investigations on the intersystem crossing between the singlet and triplet pathways are beyond experimental observations and are also challenging for theoretical approaches. Theoretical descriptions of the dirhodium-nitrene promoted C−H amination and alkene aziridination are largely less than their experimental counterparts; the spin crossover involved calculations are even rare.[6f−h,15] Harvey and collaborators suggested that there is significant spin−orbital coupling between the different spin state surfaces at the spin crossover points.[20] In this theoretical effort, the questions mentioned above are comprehensively investigated, and we try to provide a thorough understanding of the reaction mechanisms as well as the nature of the intersystem crossing.

In this present paper, three dirhodium catalysts (elaborately selected from a series of experimental reports by Du Bois and co-workers[3l,m,o]) were utilized to promote the intramolecular C−H insertion (I) and alkene aziridination (A) of 4-pentenylsulfamate (Figure 2). Dirhodium-nitrene is the starting material, and only

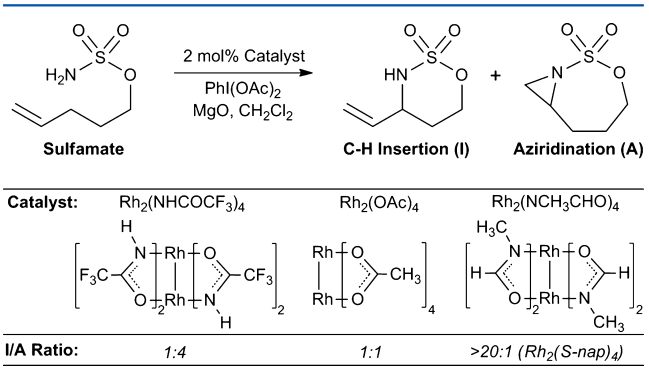

Figure 2. Intramolecular allylic C−H amination versus alkene aziridination promoted by three different dirhodium catalysts.

the product-determining C−H amination/C−N formation processes are considered. C−H amination could occur at the allylic center to give the oxathiazinane product, while alkene aziridination would form a fused 7,3-bicyclic ring product. $Rh_2(NHCOCF_3)_4$ exhibits a slight bias for the aziridination (I/A ratio is 1:4),[3m] $Rh_2(OAc)_4$ has no catalytic propensity for the two different reactions (I/A ratio is 1:1),[3m] and $Rh_2(NCH_3CHO)_4$ (a $Rh_2(S\text{-nap})_4$[3l] model catalyst, utilized in order to keep the computations tractable for our computational resources) is strongly biased toward C−H amination (I/A ratio is >20:1).[3l] In the theoretical effort, the influence of the electronic effect on chemoselectivity is mainly explored. The steric effect is also considered due to the fact that remote steric effects between the catalyst and substrate frameworks can direct reaction chemoselectivity.

COMPUTATIONAL DETAILS

All of the calculations were performed with the Gaussian 09 suite of programs.[21] Density functional (DFT) was utilized in combination with the BPW91 (the Becke's exchange functional and PW91 correlation functional)[22] and M06L (the pure functional of Truhlar and Zhao)[23] pure functionals. The BPW91 functionals, being both economical and reliable, are found to appropriately describe the singlet−triplet energy difference (E_{st}) of dirhodium−nitrene complexes.[5,6f,h,11b,c,24] Therefore, the BPW91 pure functionals were utilized to optimize reaction complexes and to obtain their corresponding energies. However, we found that the energy barriers of the alkene aziridination reactions calculated by the BPW91 functionals are always overestimated by about 5 kcal/mol, when compared with the M06L level of calculations (see farther below). The M06L pure functional was found to be accurate for the thermochemistry predictions and weak interaction descriptions for systems of both transition metals and main group elements.[23,25] Finally, the M06L pure functionals were also employed to optimize and feature key reaction species. Minimum-energy crossing points (MECPs) between singlet−triplet potential energy surfaces (PES) were located with the MECP program developed by Harvey and co-workers.[20] Che and co-workers demonstrated that the influence of different basis sets on the accuracy of energy descriptions is not obvious, and it is not necessary to use rather higher and more expensive basis sets. Therefore, 6-31G*

dx.doi.org/10.1021/jo5019987 | J. Org. Chem. XXXX, XXX, XXX−XXX

basis sets for C, H, O, N, S, and Cl light atoms, the 1997 Stuttgart relativistic small-core effective core potential (Stuttgart RSC 1997 ECP)[26] for Rh atoms (with an augment of 4f function [ζ_f(Rh) = 1.350][27]), were utilized. These composite basis sets (denoted as BS1) are shown to be effective for the assessment of rhodium-containing complexes.[6h,28] Other composite basis sets (denoted as BS2) consisting of the diffusion basis sets 6-31+G* (for C, H, O, N, S, and Cl atoms) and the same Stuttgart basis sets as in BS1 (for Rh atoms) were also employed in consideration of the significant orbital interactions between Rh and its surrounding atoms. To conclude, BPW91 in combination with BS1, or M06L combined with BS2, is utilized for geometry optimizations, harmonic vibrational frequency calculations, intrinsic reaction coordinate (IRC) calculations,[29] MECPs locations, and frontier orbital analysis. It is of note that the dirhodium-nitrene involved calculations (especially M06L level of computations) are difficult to converge. Therefore, quadratic convergence (QC) or XQC options are utilized in case the first-order SCF has not converged.

Subsequently, the single-point solvation energies of gas-phase optimized geometries in dichloromethane (Eps = 8.93) were estimated by utilizing the integral equation formalism polarized continuum model (IEFPCM) with radii and nonelectrostatic terms for Truhlar and co-workers' SMD solvation model (SMD-Coulomb).[30] Diffusion functional basis sets 6-311++G** for the C, H, O, N, S, and Cl atoms in combination with the same Stuttgart basis sets as in BS1 for Rh atoms (together denoted as BS3) were employed to perform the solvation single-point calculations. The methods utilized for the solvation energy refinement are consistent with their corresponding optimization involved methods. The free energy values reported in the present paper are in kcal/mol and in solution. Finally, natural bond orbital (NBO)[31] analysis and Milliken spin density distribution analysis using a combination of M06L/BS3 were performed on gas-phase optimized complexes to investigate the reaction mechanisms from the microscopic viewpoint. All of the thermodynamic data were obtained at 298.15 K.

RESULTS AND DISCUSSION

In the present paper, the intramolecular allylic C−H insertion (amination) versus alkene aziridination of 4-pentenylsulfamate promoted by three different dirhodium complexes are investigated. The species reported in the paper are denoted as n-^{m}ITEM$_{x\text{-}y}$, where n = 1 for $Rh_2(OAc)_4$, 2 for $Rh_2(NHCOCF_3)_4$, 3 for $Rh_2(NCH_3CHO)_4$, and 4 for Cl−$Rh_2(OAc)_4$ involved reactions; m = 1 for singlet and 3 for triplet spin state multiplicities; ITEM = RC for a reaction reactant, TS for a transition state, IM for a reaction intermediate, and PC for a product; x = I refers to the C−H insertion reactions while x = A is the alkene aziridination processes; and finally y = A, B, C... refers to different catalyst−substrate binding modes and corresponding reaction coordinates. For simplicity's sake, labels of the atoms in the active sites of reaction complexes are given (Figure 3). The optimized structures are provided in Figures S1, S2, and S3 in the Supporting Information.

a. $Rh_2(OAc)_4$ Promoted Reactions. *Catalyst−Substrate Binding Modes.* $Rh_2(OAc)_4$ is a typical paddlewheel dirhodium complex donating two facile axial coordinate sites, both or either of which can be occupied by substrate molecules. Du Bois and co-workers found that the reaction rate has first-order dependence on the sulfamate substrate.[3m] Therefore, the case in which only one axial coordinate site is occupied by a sulfamate molecule is exclusively considered in the paper. Subsequently and more importantly, the catalyst−substrate binding modes in key transition states are still not clear. Small energetic differences among different catalyst−substrate binding modes could result in disparate chemoselectivity (2 kcal/mol for >20:1 selectivity). It is necessary but very challenging to find out the most stable binding mode(s).

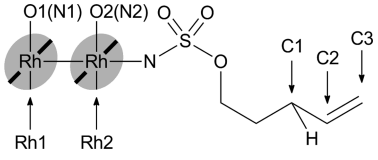

Figure 3. Depicted are labels of the atoms in the active sites of reaction complexes. O1(N2) and O2(N2) refer to the oxygen (nitrogen) atoms coordinated to Rh1 and Rh2 centers, respectively.

The catalyst−substrate binding modes of transition states involved in alkene aziridination are not well illustrated. The plane defined by a Rh center and the four carboxylate oxygen atoms coordinated with it (denoted as Rh-plane) is "isotropic", which enables various catalyst−substrate binding modes (Figure 4). The sulfamate can "stand" on (the S−O(R) bond is nearly perpendicular to the Rh-plane, denoted as Stand-mode) or "lie" on the Rh-plane (the S−O(R) bond is nearly parallel to the Rh-plane, denoted as Lie-mode); the terminal C═C bond can incline toward or away from the catalyst; both of the alkenyl-carbon centers can be electrophilicly attacked by the dirhodium-nitrene. Therefore, up to eight binding modes could be generated. Modes D and F are excluded due to their severe steric hindrance with the catalyst. Mode H is also ruled out because of its significant ring tension. Finally, six catalyst−substrate binding modes are considered in analyzing the transitions states of alkene aziridination. Of note, modes C and E are also reported by Du Bois and co-workers.[3o] The catalyst−substrate binding modes of H-abstraction involved transition states in C−H amination reactions are relatively simple and well illustrated. Only Stand-mode and Lie-mode are optional, and previous studies have demonstrated that the Stand-mode is more preferable.[3o,6f,h] Therefore, only Stand-mode (the S−O(R) bond is nearly perpendicular to the Rh-plane) is presented herein.

Mechanisms of Alkene Aziridination. As mentioned above, five different catalyst−substrate binding modes (mode A, B, C, E, and G) are considered and their proposed reaction mechanisms are provided in Figure S4 in the Supporting Information. Note that mode G is ruled out due to the fact that a five-member ring byproduct is formed according to IRC calculations performed on the singlet transition state 1-^{1}TS$_{A\text{-}G}$ (Figure S5 in Supporting Information). Similarly, a singlet concerted pathway and a triplet stepwise pathway are observed in the four remaining proposed modes A, B, C, and E. The C2 center (seen in Figure 3) is initially electrophilicly attacked by the singlet/triplet nitrenoid in modes A, B, and C, while an electrophilic attack is first observed in the terminal C3 center (seen in Figure 3) in mode E. The calculated free energy barriers of these four modes indicate that the terminal alkenyl C3 center is more inclined to be electrophilicly attacked. The regioselectivity could be ascribed to the subtle intrinsic tension of seven-member/eight-member rings. Therefore, mode E is the most favorable binding mode and only mode E is thoroughly discussed in the present paper for simplicity's sake.

The N−C3 and N−C2 distances in the singlet transition state 1-^{1}TS$_{A\text{-}E}$ (optimized by M06L/BS2) are 2.35 and 2.97 Å, respectively. The vibration of the imaginary frequency indicates a tendency for a major N−C3 bond formation vs a slight N−C2 bond formation. The N−C2 bond formation is completed in a barrier-free process followed by the transition state 1-^{1}TS$_{A\text{-}E}$. In other words, the C═C bond is directly attacked by the singlet nitrenoid. Two electrons on the $\pi_{p\text{-}p}$ bond transfer to the vacant p orbital of the singlet nitrenoid in 1-^{1}TS$_{A\text{-}E}$, which can be proved by the NBO charge change on C1, C3, and N atoms (see in Table 1) and the frontier orbital analysis (Figure 5). Therefore, it can be

dx.doi.org/10.1021/jo5019987 | J. Org. Chem. XXXX, XXX, XXX−XXX

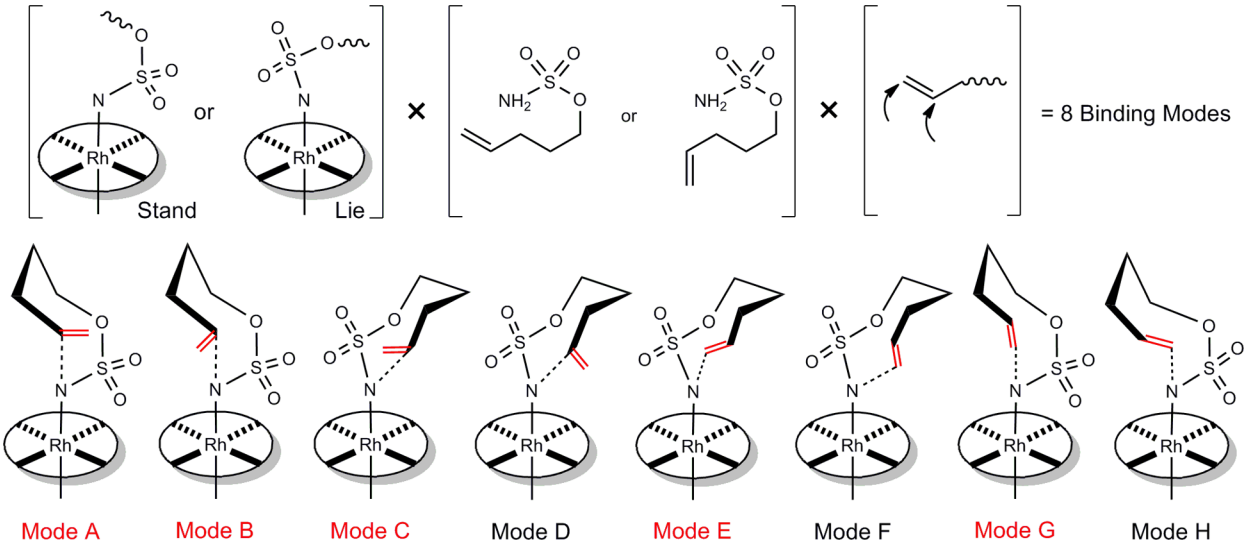

Figure 4. Depicted are eight proposed catalyst−substrate binding modes of key transition states in alkene aziridination reactions.

Table 1. Calculated NBO Charge for Selected Atoms in the Optimized Structures for the $Rh_2(OAc)_4$ Entry at the M06l/BS3 Level of Theory

structures	Rh1	Rh2	N	C1	C2	C3	C1 + C2 + C3	H	O1	O2
1-^{1}RC	0.662	0.673	−0.539	−0.402	−0.151	−0.377	−0.930	0.186	−0.59	−0.55
1-^{3}RC	0.693	0.669	−0.550	−0.404	−0.147	−0.375	−0.926	0.187	−0.59	−0.55
1-^{1}TS$_{A\text{-}E}$	0.662	0.655	−0.608	−0.405	−0.074	−0.308	−0.787	0.215	−0.59	−0.56
1-^{1}PC$_{A\text{-}E}$	0.651	0.562	−0.656	−0.397	−0.011	−0.174	−0.582	0.212	−0.59	−0.60
1-^{3}TS1$_{A\text{-}E}$	0.674	0.661	−0.626	−0.423	−0.089	−0.280	−0.792	0.209	−0.59	−0.56
1-^{3}IM$_{A\text{-}E}$	0.682	0.671	−0.677	−0.439	−0.046	−0.257	−0.742	0.202	−0.59	−0.56
1-^{3}TS2$_{A\text{-}E}$	0.727	0.672	−0.773	−0.450	0.040	−0.230	−0.640	0.217	−0.60	−0.58
1-^{3}PC$_{A\text{-}E}$	0.719	0.674	−0.688	−0.398	−0.019	−0.180	−0.597	0.210	−0.60	−0.61
1-^{1}TS$_{I\text{-}A}$	0.658	0.637	−0.708	−0.292	−0.159	−0.200	−0.651	0.292	−0.60	−0.56
1-^{1}PC$_{I\text{-}A}$	0.660	0.553	−0.797	−0.039	−0.173	−0.328	−0.540	0.402	−0.59	−0.60
1-^{3}TS1$_{I\text{-}A}$	0.687	0.667	−0.725	−0.330	−0.158	−0.321	−0.809	0.310	−0.59	−0.56
1-^{3}IM$_{I\text{-}A1}$	0.690	0.694	−0.882	−0.108	−0.274	−0.314	−0.696	0.401	−0.59	−0.55
1-^{3}TS2$_{I\text{-}A1}$	0.741	0.663	−0.946	−0.006	−0.246	−0.293	−0.545	0.383	−0.60	−0.58
1-^{3}PC$_{I\text{-}A1}$	0.729	0.660	−0.838	−0.043	−0.186	−0.333	−0.562	0.399	−0.60	−0.61
1-^{3}IM1$_{I\text{-}A2}$	0.690	0.694	−0.882	−0.108	−0.275	−0.313	−0.696	0.401	−0.59	−0.55
1-^{3}TS2$_{I\text{-}A2}$	0.681	0.682	−0.873	−0.109	−0.264	−0.303	−0.676	0.407	−0.59	−0.55
1-^{3}IM2$_{I\text{-}A2}$	0.693	0.688	−0.880	−0.101	−0.255	−0.310	−0.666	0.391	−0.59	−0.56
1-^{3}TS3$_{I\text{-}A2}$	0.741	0.666	−0.950	−0.005	−0.259	−0.266	−0.530	0.375	−0.60	−0.57
1-^{3}PC$_{I\text{-}A2}$	0.727	0.674	−0.838	−0.044	−0.180	−0.318	−0.542	0.394	−0.60	−0.60

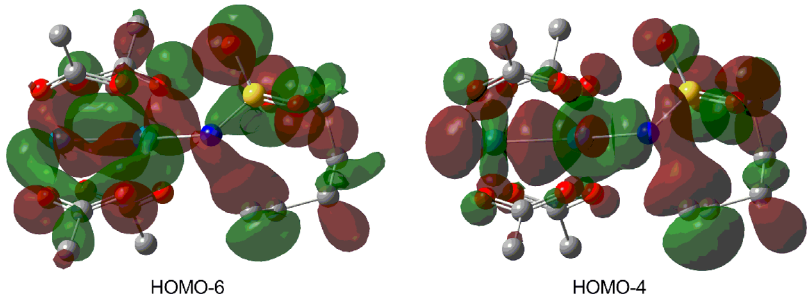

Figure 5. Kohn−Sham frontier orbitals (isovalue: 0.10) of the transition state 1-^{1}TS$_{A\text{-}E}$.

concluded that the singlet alkene aziridination is also a concerted, highly asynchronous electrophilic oxidation process.

The triplet alkene aziridination pathway is also investigated. The C3 center is electrophilicly attacked by the triplet nitrenoid in 1-^{3}TS1$_{A\text{-}E}$. Inspection of Table 2 shows that the Mulliken spin density on the C2 center increases from 0.008 in 1-^{3}RC to 0.503 in 1-^{3}TS1$_{A\text{-}E}$, which indicates a hemolytic cleavage of the $\pi_{p\text{-}p}$ bond and one electron is attracted by the single-electron p orbital of the triplet nitrenoid to form the N−C(3) bond, while the other one resides on the C2 center. Therefore, a diradical

dx.doi.org/10.1021/jo5019987 | J. Org. Chem. XXXX, XXX, XXX−XXX

Table 2. Mulliken Atomic Spin Densities for Selected Atoms in the Optimized Structures for the $Rh_2(OAc)_4$ Entry at the M06l/BS3 Level of Theory

structures	Rh1	Rh2	N	C1	C2	C3	O1	O2
1-^{3}RC	0.345	0.309	1.065	0.014	0.008	0	−0.002	0.058
1-^{3}TS1$_{A-E}$	0.277	0.292	0.870	−0.020	0.503	−0.100	0.001	0.039
1-^{3}IM$_{A-E}$	0.236	0.277	0.444	−0.028	1.048	−0.107	0.003	0.016
1-^{3}TS2$_{A-E}$	0.699	0.687	−0.008	−0.033	0.520	−0.019	0.055	0.070
1-^{3}PC$_{A-E}$	0.856	0.929	0.036	−0.004	0.015	−0.003	0.078	0.080
1-^{3}TS1$_{I-A}$	0.295	0.237	0.819	0.397	−0.160	0.333	0.004	0.059
1-^{3}IM$_{I-A1}$	0.277	0.271	0.333	0.769	−0.364	0.737	0.000	0.046
1-^{3}TS2$_{I-A1}$	0.717	0.634	−0.020	0.307	−0.085	0.317	0.060	0.082
1-^{3}TS2$_{I-A2}$	0.240	0.258	0.411	0.736	−0.340	−0.733	0.001	0.044
1-^{3}IM2$_{I-A2}$	0.295	0.312	0.303	0.693	−0.304	0.732	0.002	0.027
1-^{3}TS3$_{I-A2}$	0.699	0.691	−0.001	0.381	−0.112	0.309	0.053	0.049

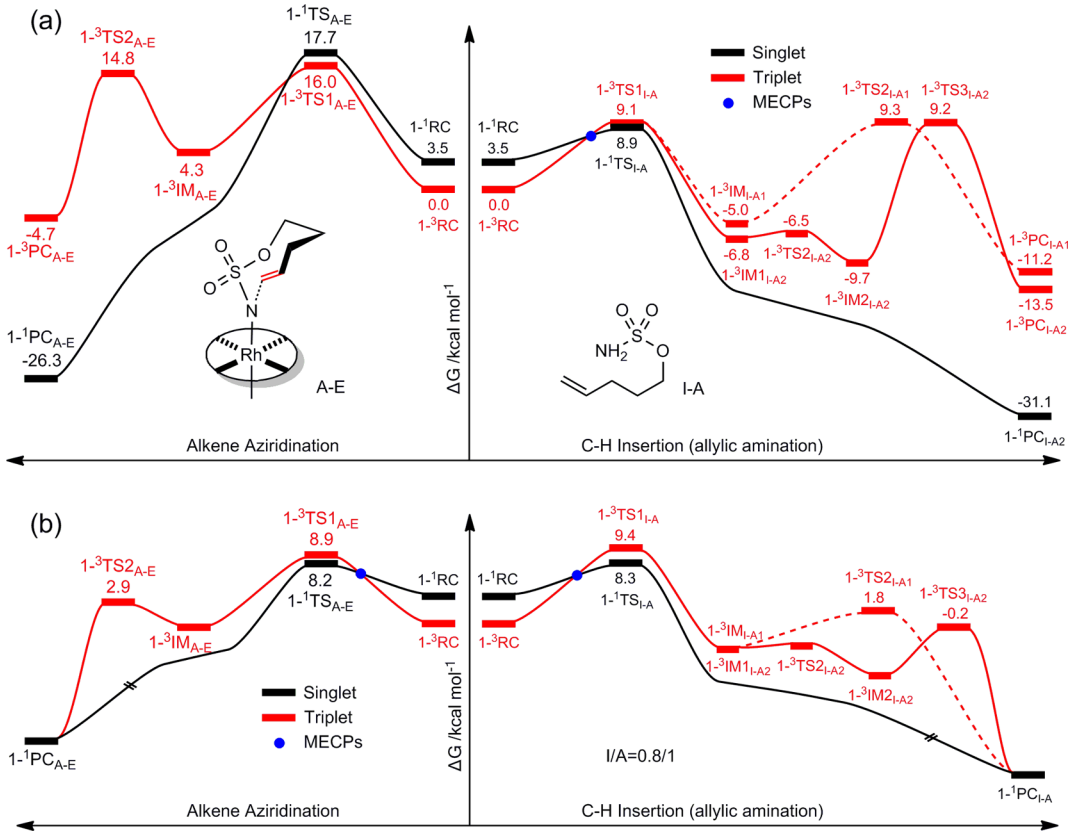

Figure 6. Depicted are the potential energy surface (PES) profiles of the intramolecular allylic C−H amination versus alkene aziridination promoted by the $Rh_2(OAc)_4$: (a) calculated at the level of BPW91/BS1; (b) calculated at the level of M06L/BS2. The I/A ratio calculated by the M06L/BS2 is 0.8/1. The locations of MECPs are similar to those found in our previous work.[6h] Detailed discussion of the location and nature of MECPs is provided in ensuing sections.

intermediate 1-^{3}IM$_{A-E}$ is observed with the spin densities on N and C2 atoms as 0.444 and 1.048, respectively. Subsequently, the diradical-rebound N−C(2) formation is observed in 1-^{3}TS2$_{A-E}$, and finally the triplet product 1-^{3}PCA-E is obtained. The potential energy surface (PES) profiles of the A-E pathway are depicted in Figure 6.

Mechanisms of C−H Amination. As mentioned above, the C═C bond could incline toward (denoted as I-A) or away from (denoted as I-B) the catalyst, which may lead to energetic differences in the optimized structures. Therefore, four reaction pathways (considering singlet−triplet spin states) are proposed in accordance with the two C═C bond orientations (Figure S6 in Supporting Information). The chains of 4-pentenylsulfamate in dirhodium-nitrene reactants 1-^{1}RC and 1-^{3}RC are both inclined away from the dirhodium catalysts. First, a singlet concerted H-abstraction/C−N formation pathway is obtained. The vibration corresponding to the unique imaginary frequency in either 1-^{1}TS$_{I-A}$ or 1-^{1}TS$_{I-B}$ shows a clear process for H-abstraction and no evidence of C−N formation. The IRC calculations performed on both 1-^{1}TS$_{I-A}$ and 1-^{1}TS$_{I-B}$ also indicate a concerted, highly asynchronous pathway. Inspection of Table 1 shows that the total charge of the C1−C2−C3 moiety varies significantly from −0.930 for 1-^{1}RC to −0.651 for 1-^{1}TS$_{I-A}$, indicative of a heterolytic cleavage of the C−H bond and the subsequent hydride-transfer character of the H-abstraction process in 1-^{1}TS$_{I-A}$.

dx.doi.org/10.1021/jo5019987 | J. Org. Chem. XXXX, XXX, XXX−XXX

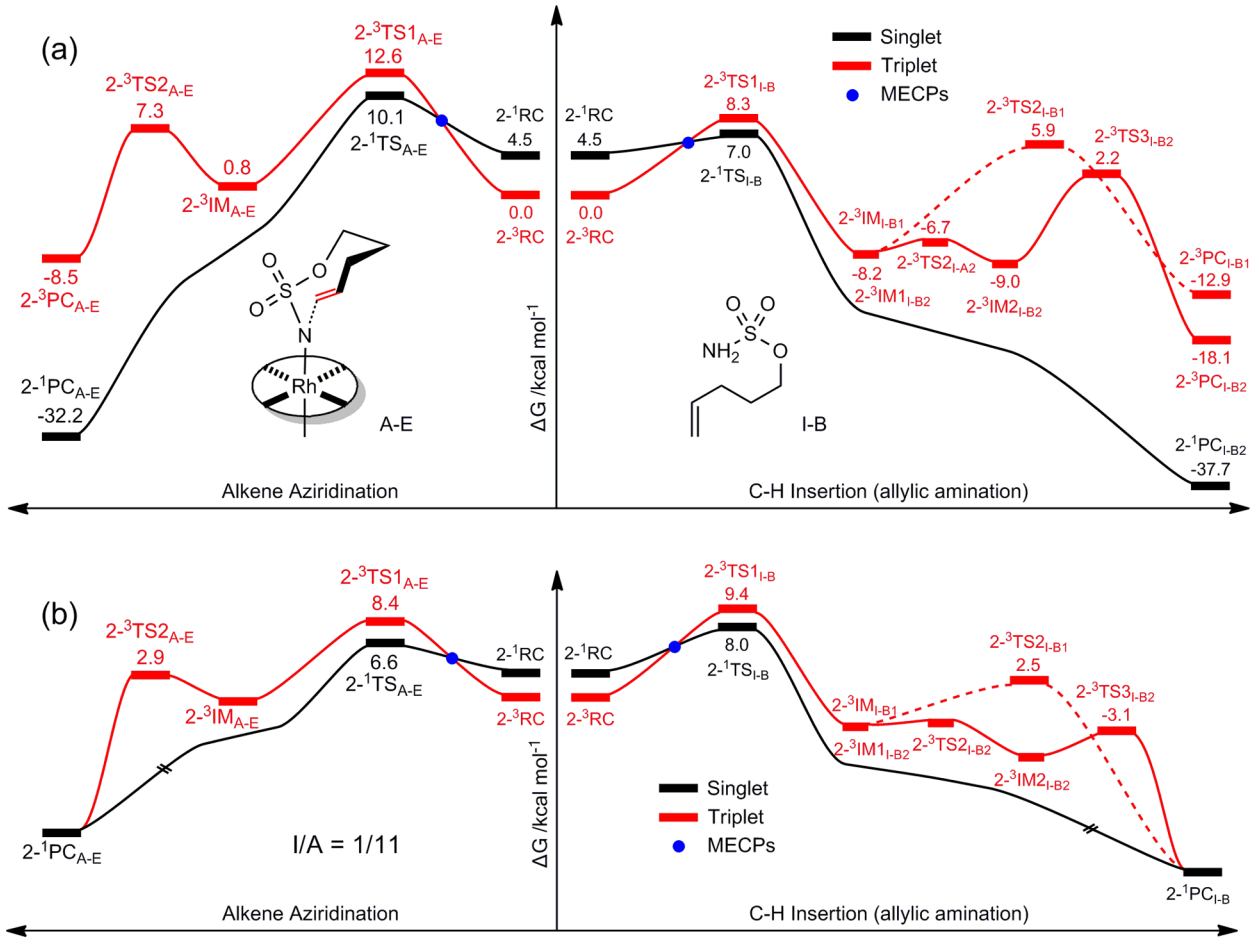

Figure 7. Depicted are the potential energy surface (PES) profiles of the intramolecular C−H amination versus alkene aziridination promoted by the $Rh_2(NHCOCF_3)_4$: (a) Calculated at the level of BPW91/BS1; (b) Calculated at the level of M06L/BS2. The I/A ratio calculated by the M06L/BS2 is 1/11.

In contrast, a triplet stepwise H-abstraction/C−N formation pathway is also located. Both 1-^{3}TS1$_{I-A}$ and 1-^{3}TS1$_{I-B}$ involve a complete H-abstraction process, and the optimized geometries are quite similar to their singlet counterparts. The variation in total charge of C1−C2−C3 from 1-^{3}RC to 1-^{1}TS$_{I-A}$ is not obvious (−0.926 for 1-^{3}RC and −0.809 for 1-^{1}TS$_{I-A}$). The spin density of the C1−C2−C3 moiety increases significantly from 0.022 for 1-^{3}RC to 0.570 for 1-^{1}TS$_{I-A}$ (see in Table 2). Both NBO charge distribution and Mulliken spin density analysis are indicative of a C−H hemolytic cleavage and then hydrogen-migration character of the H-abstraction process in 1-^{3}TS1$_{I-A}$. The hemolytic cleavage of the C−H bond in 1-^{3}TS1$_{I-A}$ results in two diradical intermediates 1-^{3}IM$_{I-A1}$ and 1-^{3}IM1$_{I-A2}$. 1-^{3}IM$_{I-A1}$ and 1-^{3}IM1$_{I-A2}$ are structurally similar but lead to different C−N formation patterns. The configurations of the N and allylic C1 centers in 1-^{3}IM$_{I-A1}$ are planar structures, and the total spin densities for the Rh1−Rh2−N and C1−C2−C3 moieties are 0.881 and 1.142, respectively. Therefore, it can be concluded that 1-^{3}IM$_{I-A1}$ is a triplet diradical intermediate. Subsequently, the diradical-rebound C−N formation process is observed in 1-^{3}TS2$_{I-A1}$ and finally a triplet product 1-^{3}PC$_{I-A1}$ is obtained. However, the diradical recombination is not directly connected to the triplet intermediate 1-^{3}IM1$_{I-A2}$. A N−H swing transition state 1-^{3}TS2$_{I-A2}$ is observed instead. The H−S−Rh2−N dihedral angle from 1-^{3}IM1$_{I-A2}$ to 1-^{3}TS2$_{I-A2}$ to 1-^{3}IM2$_{I-A2}$ is gradually changed (1.1° for 1-^{3}IM1$_{I-A2}$, −3.6° for 1-^{3}TS2$_{I-A2}$, and −16.7° for 1-^{3}IM2$_{I-A2}$). The N−H bond swing process in 1-^{3}TS2$_{I-A2}$ results in another intermediate 1-^{3}IM2$_{I-A2}$. The configuration of the N atom in 1-^{3}IM2$_{I-A2}$ is a planar-pyramidal mixture, which is strongly prone to precede C−N formation at the spatial abundant side of the N-radical. Subsequently, a diradical-rebound C−N formation is observed in 1-^{3}TS3$_{I-A2}$ and the other triplet product 1-^{3}PC$_{I-A2}$ is obtained. 1-^{3}PC$_{I-A1}$ and 1-^{3}PC$_{I-A2}$ are racemic products, and the singlet product 1-^{1}PC$_{I-A2}$ shares the same chirality with 1-^{3}PC$_{I-A2}$. In a previous work by Che and collaborators,[5] the C−C bond rotation is assumed to be the reason for the formation of racemic products. However, their assumption lacks experimental and computational support. We believe that it is the N−H bond swing not the C−C bond rotation that leads to racemic products. The diradical-rebound C−N formation process calculated in the paper requires an ∼15 kcal/mol (BPW91/BS1 calculated) or much smaller (M06L/BS2 calculated) reaction barrier, which then supports the idea that the diradical-recombination C−N formation process indeed has an identifiable energy barrier.[6h,13] To conclude, the singlet pathway is observed in a concerted, highly asynchronous manner; only the hydride-transfer process is observed in the transition state and obtains an enantiomerically pure product. Oppositely, the triplet pathway is a typical stepwise mechanism in which the hydrogen-migration process and C−N formation are involved in different transition states. More

dx.doi.org/10.1021/jo5019987 | J. Org. Chem. XXXX, XXX, XXX−XXX

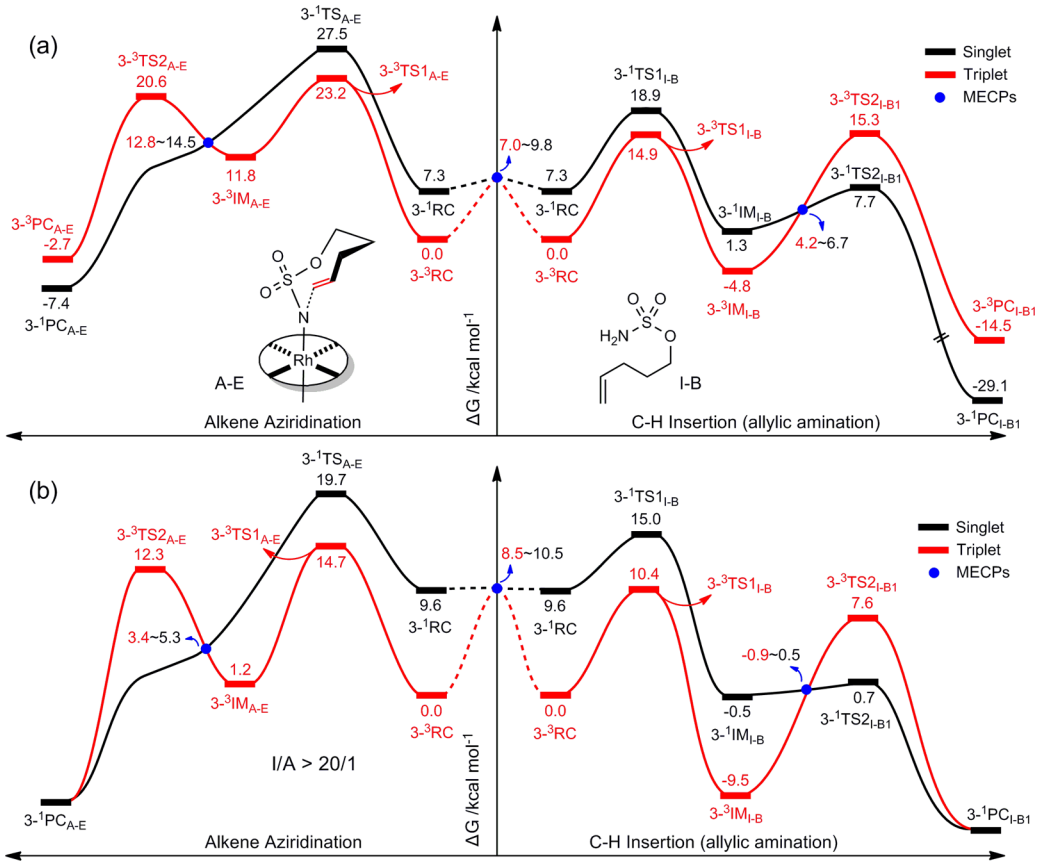

Figure 8. Depicted are the potential energy surface (PES) profiles of the intramolecular C−H amination versus alkene aziridination promoted by the $Rh_2(NCH_3CHO)_4$: (a) Calculated at the BPW91/BS1 level; (b) calculated at the M06L/BS2 level. The I/A ratio calculated by the M06L/BS2 level is >20/1.

importantly, the possibility of a N−H bond swing transition state leads to a racemic product.

Meanwhile, it can be found that the I-A involved pathway (the C═C bond incline toward the catalyst) and the I-B one (the C═C bond inclines away from the catalyst) are similar and their energetic differences are quite small. Therefore, only one C═C orientation is considered in the following entries. The PES profiles of the I-A pathway are depicted in Figure 6.

Inspection of Figure 6 shows that BPW91 can, on one hand, provide accurate optimized geometries and corresponding reactions coordinates but, on the other hand, overestimate the energy barrier of alkene aziridination. The singlet−triplet energy differences (E_{st}) of C−H amination and alkene aziridination are small (within 1.7 kcal/mol), and the singlet and triplet pathways stay competitive. The singlet pathway is slightly more competitive, and the chemoselectivity on C−H insertion (I) and alkene aziridination (A) is calculated by eq 1 with a value of 0.8:1, which is very close to the experimentally observed value (the I/A ratio = 1/1).[3m]

$$\frac{I}{A} = \frac{C_I}{C_A} = \frac{\Sigma \exp(-\Delta G_I^{\neq}/RT)}{\Sigma \exp(-\Delta G_A^{\neq}/RT)} \quad (1)$$

b. $Rh_2(NHCOCF_3)_4$ Promoted Reactions. Tetra-carboxamidates possess different electronic and steric effects from the tetra-carboxylate ligands, and in this part, the intramolecular C−H insertion versus alkene aziridination promoted by the $Rh_2(NHCOCF_3)_4$ complex is investigated. The dirhodium tetra-carboxamidates complexes emerge in multiple isomers, but the *cis*-2,2 isomer in which two nitrogen atoms and two oxygen atoms coordinate with each rhodium center with the two nitrogens cis is dominant.[1d] Therefore, only the *cis*-2,2 isomers of the $Rh_2(NHCOCF_3)_4$ and $Rh_2(NCH_3CHO)_4$ complexes are considered in the paper.

The *cis*-2,2 isomer of $Rh_2(NHCOCF_3)_4$ possesses two N−H sites that are available for intermolecular hydrogen bonds. Therefore, the possible catalyst−substrate binding modes in the $Rh_2(NHCOCF_3)_4$ involved reactions are reduced and the most stable one is featured in two significant N−H···O(R) intermolecular hydrogen bonds between the catalyst and the sulfamate substrate.

Similar to the $Rh_2(OAc)_4$ promoted reactions, mode E in which the terminal olefin C3 center is initially electrophilicly attacked by the nitrenoid is more favorable. The I-B orientation in which the C═C bond is inclined away from the dirhodium-nitrene is considered in the C−H amination process. The obtained reaction mechanisms are similar to the $Rh_2(OAc)_4$ involved ones. A singlet concerted, highly asynchronous pathway and an alternate triplet stepwise pathway are obtained in either the C−H amination or alkene aziridination reaction promoted by the $Rh_2(NHCOCF_3)_4$ complex. The proposed reaction pathways are depicted in Figure 7. Inspection of Figure 7 shows that the BPW91 functional again provides an accurate singlet−triplet energy difference but overestimates the energy barriers of alkene aziridination. The calculated singlet−triplet energy differences (E_{st}) in $Rh_2(NHCOCF_3)_4$ promoted reactions are slightly larger than those in $Rh_2(OAc)_4$ systems. The singlet pathways are more competitive than their triplet counterparts and the calculated I/A

dx.doi.org/10.1021/jo5019987 | J. Org. Chem. XXXX, XXX, XXX−XXX

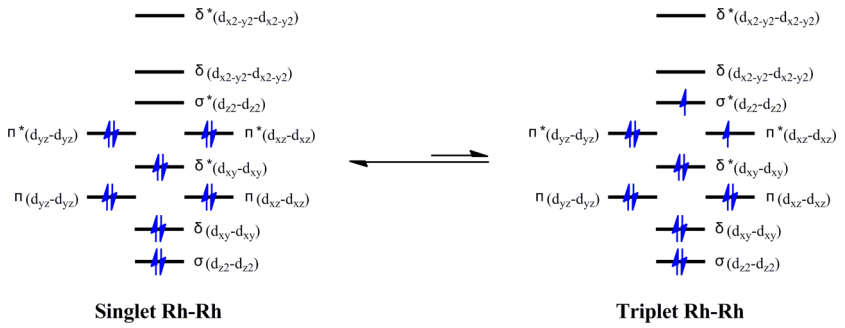

Figure 9. Depicted is the possible spin change of the singlet−triplet dirhodium center.

Table 3. Relative Free Energies (Optimized by BPW91/BS1) of Reaction Species in $Rh_2(OAc)_4$ and Cl−$Rh_2(OAc)_4$ Promoted Reactions

	1-^3RC	1-^1RC	$1\text{-}^1TS_{A\text{-}E}$	$1\text{-}^3TS1_{A\text{-}E}$	$1\text{-}^3IM_{A\text{-}E}$	$1\text{-}^3TS2_{A\text{-}E}$	$1\text{-}^1TS_{I\text{-}A}$	$1\text{-}^3TS1_{I\text{-}A}$	$1\text{-}^3IM_{I\text{-}A}$	$1\text{-}^3TS2_{I\text{-}A1}$
ΔG (kcal/mol)	0.0	3.5	17.7	16.0	4.3	14.8	8.9	9.1	−6.8	9.3
	4-^3RC	4-^1RC	$4\text{-}^1TS_{A\text{-}E}$	$4\text{-}^3TS1_{A\text{-}E}$	$4\text{-}^3IM_{A\text{-}E}$	$4\text{-}^3TS2_{A\text{-}E}$	$4\text{-}^1TS_{I\text{-}A}$	$4\text{-}^3TS1_{I\text{-}A}$	$4\text{-}^3IM_{I\text{-}A}$	$4\text{-}^3TS2_{I\text{-}A1}$
ΔG (kcal/mol)	0.0	6.2	20.5	20.0	6.8	20.5	12.8	12.7	−7.5	17.9

ratio is 1/11, which is in good agreement with the experimental value (1/4).[3m]

By referring to Figures 6 and 7, it is interesting to find that the enantiomerically pure product obtained from the singlet pathway shares the same chirality with the triplet product generated from the pathway with a relatively lower energy barrier of the diradical-rebound C−N formation (such as $1\text{-}^1PC_{I\text{-}A2}$ and $1\text{-}^3PC_{I\text{-}A2}$, 2-^1PC_{I-B2} and 2-^3PC_{I-B2}). Is that a coincidence or indicative of something unified for singlet−triplet pathways? Is it possible to find a stepwise singlet pathway? Furthermore, the nature of singlet−triplet pathways could be illuminated if a universal mechanism is provided. Further mechanistic investigation was undertaken.

c. $Rh_2(NCH_3CHO)_4$ Promoted Reactions. The tetracarboxamidates in the $Rh_2(NHCOCF_3)_4$ complex are poor electron-donating ligands and in this part, the intramolecular allylic C−H amination versus alkene aziridination is promoted by the good electron-donating $Rh_2(NCH_3CHO)_4$ complex. Similar to $Rh_2(NHCOCF_3)_4$, only the *cis*-2,2 isomer of $Rh_2(NCH_3CHO)_4$ is considered in the present paper. The methyl groups on the two nitrogens cis are bulky, which then reduces the possibilities of the catalyst−substrate binding modes. Similarly, mode E in which the substrate lies on half of the Rh-plane and the other half is occupied by the two methyl groups is considered to be most favorable. The proposed mechanisms of alkene aziridination are similar to the $Rh_2(OAc)_4$ and $Rh_2(NCH_3CHO)_4$ promoted ones. A singlet concerted, high asynchronous pathway and a triplet stepwise pathway are obtained. However, the C−H amination mechanisms are different. The triplet pathway is also a stepwise mechanism involving hydrogen migration/diradical-recombination C−N formation processes. The singlet pathway is no longer concerted but presents in an interesting and fascinating stepwise mechanism (the NBO charge is provided in Table S1 in Supporting Information). The total charge of the C1−C2−C3 moiety is gradually getting positive from −0.942 for 3-^1RC, to −0.809 for 3-^1TS1_{I-B}, to −0.598 for 3-^1IM_{I-B1}, and to −0.565 for 3-^1TS2_{I-B1}. The charge of the N atom, on the other hand, becomes increasingly negative. The NBO charge distribution analysis shows that the existence of the heterolytic cleavage of C−H bond in the hydride transfer transition state 3-^1TS1_{I-B} and a carbocation center is observed in intermediate 3-^1IM_{I-B1}. Subsequently, the positive allylic C1 center is nucleophilicly attacked by the two-electron p orbital of the N atom in 3-^1TS2_{I-B1} and finally 3-^1PC_{I-B1} is obtained. The I−B1 insertion is more competitive than the I−B2 in both singlet and triplet pathways (see in Figure S7 in Supporting Information). The simplified PES profiles of the intramolecular allylic C−H amination versus alkene aziridination are depicted in Figure 8.

By referring back to Figures 6 and 7, singlet pathways are relatively more competitive in both $Rh_2(OAc)_4$ and $Rh_2(NHCOCF_3)_4$ promoted reactions. However, Figure 8 shows that triplet pathways are initially more favorable than their singlet counterparts in the $Rh_2(NCH_3CHO)_4$ case. Significant MECPs are located before the C−N formation processes (the C−N formation in C−H amination and C(2)−N formation in alkene aziridination). By referring back to the Mulliken spin density analysis in Table 2, the spin densities on the dirhodium center increase in the C−N formation processes and the spin densities majorly reside on the dirhodium center in their corresponding triplet products. There is significant spin−orbital coupling in the dirhodium metal center (Figure 9). One electron in the $\pi^*(d_{xz}-d_{xz}$ or $d_{yz}-d_{yz})$ orbital has to jump to the $\sigma^*(d_{z^2}-d_{z^2})$ orbital in order to maintain spin conservation, which is not necessary and energy consuming. Therefore, MECPs are located right before the triplet C−N formation process and singlet products are finally obtained. Therefore, the favored pathway of C−H amination promoted by the $Rh_2(NCH_3CHO)_4$ should be an initial triplet H-abstraction (hydrogen migration) process which then converts to a singlet C−N formation process. The reasonable alkene aziridination pathways in $Rh_2(NCH_3CHO)_4$ promoted reactions also go through a triplet C(3)−N formation process and then convert to singlet pathways. Further discussion of singlet−triplet energy differences and the nature of MECPs are provided in the following sections.

d. Cl−$Rh_2(OAc)_4$ Promoted Reactions. As mentioned above, the dirhodium paddlewheel complex $Rh_2(OAc)_4$ has two facile axial coordinate sites, which can be both or half occupied. The three entries mentioned above consider the possibilities of half-occupied conditions. However, Du Bois and collaborators found that both of the axial coordinate sites should be occupied

dx.doi.org/10.1021/jo5019987 | J. Org. Chem. XXXX, XXX, XXX−XXX

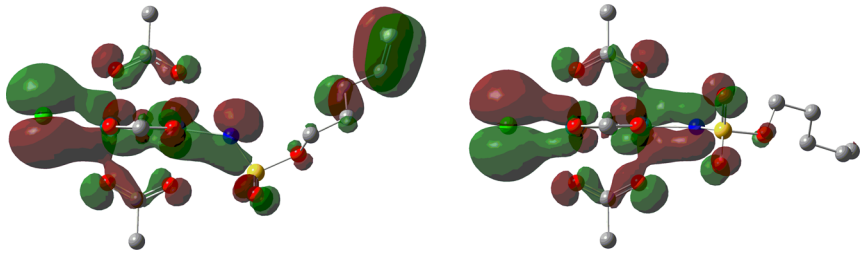

Figure 10. Kohn–Sham frontier orbitals (isovalue: 0.10) of 4-^{3}RC.

Table 4. Mulliken Atomic Spin Densities for Selected Atoms in the Reaction Reactant Complexes at the M06l/BS3 Level of Theory

structures	Rh1	Rh2	N	C1	C2	C3	H	O1	N1	O2	N2
1-^{3}RC	0.345	0.309	1.065	0.014	0.008	0.001	−0.003	−0.002	–	0.058	–
2-^{3}RC	0.499	0.130	0.874	0.000	0.013	−0.001	−0.001	0.086	0.087	0.104	0.148
3-^{3}RC	0.477	0.212	0.821	0.000	−0.001	0.000	0.000	0.091	0.099	0.312	0.140

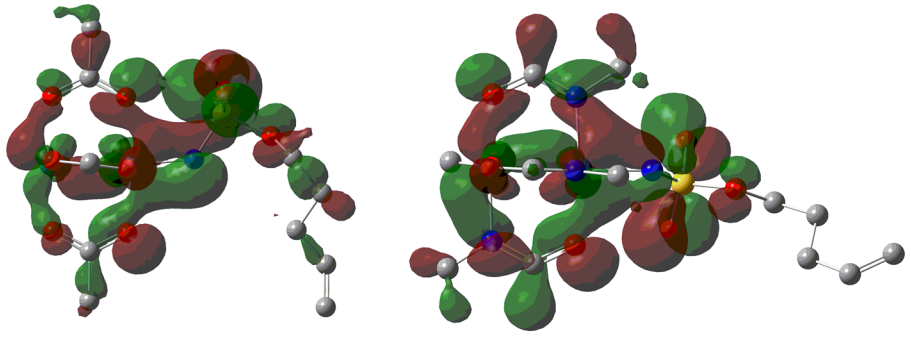

HOMO-8 (1-^{3}RC) HOMO-9 (3-^{3}RC)

Figure 11. Kohn–Sham frontier orbitals (isovalue: 0.10) of HOMO-8 in 1-^{3}RC and HOMO-9 in 3-^{3}RC.

by a substrate and an anion (such as a chloride).[3o] In principle, the electronic effects of both or half occupied entries are different and it is necessary and meaningful to conduct a further analysis and comparison. Therefore, the Cl–$Rh_2(OAc)_4$ promoted reactions are explored in the present theoretical approach. Similarly, the favorable mode E for alkene aziridination reactions is utilized and only the I-A pathway for C–H amination is considered for simplicity. The obtained reaction pathways are similar to the $Rh_2(OAc)_4$ promoted ones, and the relative free energies of reaction species in $Rh_2(OAc)_4$ and Cl–$Rh_2(OAc)_4$ involved reactions are provided in Table 3. Inspection of Table 3 shows that the reaction barriers of rate-determining steps in the Cl–$Rh_2(OAc)_4$ promoted reactions are ∼3 kcal/mol higher than those in the $Rh_2(OAc)_4$ system. As has been discussed above, the rate-determining step in either the C–H amination (the H-abstraction step) or alkene aziridination (C(3)–N foramtion) reaction is a electrophilic attack process. Better electron-donor groups will raise the energy barriers. Therefore, the chloride coordinated to the dirhodium center acts as an electron-donor group. Significant orbital interactions are observed between the Cl p_x/p_y and Rh–Rh d_{xz}–d_{xz}/d_{yz}–d_{yz} (see in Figure 10). To conclude, the reaction barriers and corresponding chemoselectivity on C–H amination and alkene aziridination could be changed via adding simple anions. This kind of reagent-controlled method can be convenient and easily conducted and may provide a deft approach to selective C–H amination and alkene aziridination. Further discussions about the functions of the rhodium(II) coordinated chloride are provided in the following sections.

e. Singlet–Tripet Energy Differences and Energy Barriers. The electronic effect is majorly considered in this report. By referring back to Figures 6, 7, and 8, the triplet reactants are more stable than their singlet counterparts. The phenomenon is ascribed to Hund's rule that the two unbonded electrons of the nitrene tend to reside in two degenerate p_x and p_y orbitals. However, significant backbonding interactions between the Rh–Rh d_{xz}–d_{xz}/d_{yz}–d_{yz} and the N p_x/p_y orbitals lead to an energy difference between the initially degenerate p_x and p_y orbitals. The free energy differences between the singlet–triplet reaction reactants (E_{st}) in the above four entries are 3.5 kcal/mol for $Rh_2(OAc)_4$, 4.5 kcal/mol for $Rh_2(NHCOCF_3)_4$, 7.3 kcal/mol for $Rh_2(NCH_3CHO)_4$, and 6.2 kcal/mol for Cl–$Rh_2(OAc)_4$. Carboxamidates are better electron donors than the carboxylate groups and the strongly donating carboxamidates groups increase the capacity of the dirhodium centers for backbonding to the π-acidic nitrene ligand, which then results in relatively larger singlet–triplet energy differences. The chloride is proved to be an electron donor, and the obtained E_{st} is relatively large.

The Mulliken atomic spin densities for the stable triplet reactants are also provided in Table 4. Inspection of Table 4 shows that the two unpaired electrons majorly reside on the N atom and Rh_2^{4+} center. Significant orbital interactions are observed between the Rh–Rh d_{xz}–d_{xz}/d_{yz}–d_{yz} and the N p_x/p_y orbitals, which accounts for substantial spin densities residing on the dirhodium center. Besides, considerable spin densities are observed on the O2/N2 atoms (bound to Rh2 center) in carboxamidates systems (2-^{3}RC and 3-^{3}RC) while negligible spin densities reside on the O2 atoms in 1-^{3}RC (0.058 in total). The differences in spin density distribution could be explained by

dx.doi.org/10.1021/jo5019987 | J. Org. Chem. XXXX, XXX, XXX–XXX

Kohn−Sham frontier orbitals (see in Figure 11). Inspection of Figure 11 shows that the orbital interactions among O2(N2) p_x/p_y, Rh2 d_{xz}/d_{yz}, and N p_x/p_y are relatively stronger in carboxamidates systems. Therefore, spin densities could easily reside on the O2/N2 atoms in 2-^{3}RC and 3-^{3}RC, which in turn stabilize the triplet reactants. That is why 3-^{3}RC possesses the largest singlet−triplet energy difference in the four triplet reactants.

The influence of electronic effect on energy barriers is also explored, and the calculated free energy barriers in the above four entries are provided in Table 5. It can be seen from Table 5 that

Table 5. Relative Free Energy Barriers (in kcal/mol) in Singlet and Triplet Pathways for the Four Entries at the BPW91/BS1 Level of Theory

	C−H insertion (I)		alkene aziridination (A)	
entries	singlet	triplet	singlet	triplet
$Rh_2(OAc)_4$	8.9	9.1	17.7	16.0
$Rh_2(NHCOCF_3)_4$	7.0	8.3	10.1	12.6
$Rh_2(NCH_3CHO)_4$	18.9	14.9	27.5	23.2
$Cl-Rh_2(OAc)_4$	12.8	12.7	20.5	20.0

the relative free energy barriers increase with a rise in electron-donor capacity of the catalysts. The rate-determining step in either the C−H amination process or the alkene aziridination reaction is essentially an electrophilic attack process. The increasing capacity of backbonding to the nitrenoid is adverse to the following electrophilic attack steps. Similar to the stabilization of triplet reactants, the strongly donating carboxamidate groups also better stabilize the triplet reaction species, and then, the triplet pathway is initially dominant in $Rh_2(NCH_3CHO)_4$ promoted reactions. The last but most important thing is the influence of electronic effect on chemoselectivity over C−H amination versus alkene aziridination. Inspection of Table 5 shows that the alkene aziridination reaction is preferable in the case of weak electron-donor catalysts, such as the $Rh_2(NHCOCF_3)_4$. Compared with the hydrogen/hydride target in C−H amination, the electron-sufficient π-bond is more sensitive to the change of electron density on the nitrenoid. Strongly electron-donating ligands result in the high electron density of the nitrene and resultant high energy barrier in the subsequent electrophilic attack step in the alkene aziridination reaction.

f. Nature of MECPs. By referring back to Figures 6, 7, and 8, three types of MECPs are located. The first type (located before the reactants) acts as a nitrene precursor. It is speculated to be the direct product of the fast elimination of PhI from metal-phenyliodinane. The singlet−triplet nitrenoids are energetically identical in that very moment, but the life of this kind of MECP would not be long. The second type of MECP is found to locate before the rate-determining step (the H-abstraction step for C−H amination or the C(3)−N formation in alkene aziridination), as demonstrated in Figures 6 and 7. In the conditions, a singlet pathway is preferred so that the stable triplet reactant would go through the MECPs and then follow the singlet reaction coordinate. Finally, the third type of MECP is observed in Figure 8, and it has been discussed above. The first and second types of MECPs are also described in previous works.[6g,h,15] To our knowledge, it is the first theoretical evidence of the third type of MECP.

g. Nature of C−H Amination and Alkene Aziridination Reaction Mechanisms. As discussed above, the singlet pathway of the C−H amination in either $Rh_2(OAc)_4$ or $Rh_2(CHCOCF_3)_4$ entry is a concerted, highly asynchronous process. Oppositely, a singlet stepwise pathway is operative in the $Rh_2(NCH_3CHO)_4$ entry. Besides, the singlet product shares the same chirality with the triplet product generated from the pathway with a relatively lower energy barrier of the diradical-rebound C−N formation. Considering the two aspects together, we reasonably and boldly estimate that the nature of the C−H amination mechanism is a stepwise process (see in Scheme 1). Strongly electron-donating catalysts (such as the $Rh_2(NCH_3CHO)_4$) can well stabilize the carbocation involved intermediates and the subsequent C−N formation transition states.

Similarly, the general mechanisms of the alkene aziridination reactions are provided and demonstrated in Scheme 2. Compared with the C−H amination processes, no stepwise pathways are observed in the singlet alkene aziridination reactions. However, we believe that the nature of the alkene aziridination reactions is also a stepwise process. Compared with the diradical-rebound C−N formation process, the combination of a carbocation and an electron-sufficient nitrogen atom is much faster. The carbocation and nitrogen atom in alkene aziridination reactions locate in a close distance, which further fasten the combination and may present in a barrier-free process. Thereby, only concerted, highly asynchronous singlet alkene aziridination pathways are obtained.

■ CONCLUDING REMARKS

The chemoselectivity on intramolecular allylic C−H amination versus alkene aziridination of sulfamate promoted by three different dirhodium paddlewheel complexes are investigated in the present paper by a DFT approach. The catalyst−substrate binding modes are systematically explored, and the results show that the sulfamate substrate tends to lie on the Rh-plane (the S−O(R) bond is nearly parallel to the Rh-plane) in the alkene aziridination reactions or stand on the Rh-plane in C−H amination processes (the S−O(R) bond is nearly perpendicular to the Rh-plane).

The proposed pathways in the dirhodium tetra-carboxylate ($Rh_2(OAc)_4$) entry and a weak electron-donating dirhodium tetra-carboxamidate ($Rh_2(CHCOCF_3)_4$) entry are similar. A singlet concerted, highly asynchronous pathway and an alternate triplet stepwise pathway are obtained in either the C−H amination process or the alkene aziridination reactions. The rate-determining step in the C−H amination reaction is a H-abstraction process, which presents as a hydride transfer in the singlet pathway compared to a hydrogen migration in the triplet pathway. The diradical-rebound C−N formation in the triplet pathway involves an identical energy barrier. The C(3)−N formation and the C(2)−N formation processes in the triplet alkene aziridination reactions are observed successively in the electrophilic attack involved transition states. The singlet pathway in either the C−H amination process or the alkene aziridination reactions promoted by the two poor electron-donating catalysts is more favorable, and the stable triplet reactants would first convert to singlet spin states by the MECPs located before the rate-determining steps and then follow the singlet reaction coordinates.

A singlet stepwise C−H amination pathway is observed in the strongly donating dirhodium tetra-carboxamidate promoted reaction (the $Rh_2(NCH_3CHO)_4$ entry). The heterolytic cleavage of the C−H bond in the rate-determining H-abstraction transition state results in an allylic carbocation and an electron-

dx.doi.org/10.1021/jo5019987 | J. Org. Chem. XXXX, XXX, XXX−XXX

Scheme 1. Universal Reaction Mechanisms of the Dirhodium Catalyzed Intramolecular Allylic C−H Amination Reactions

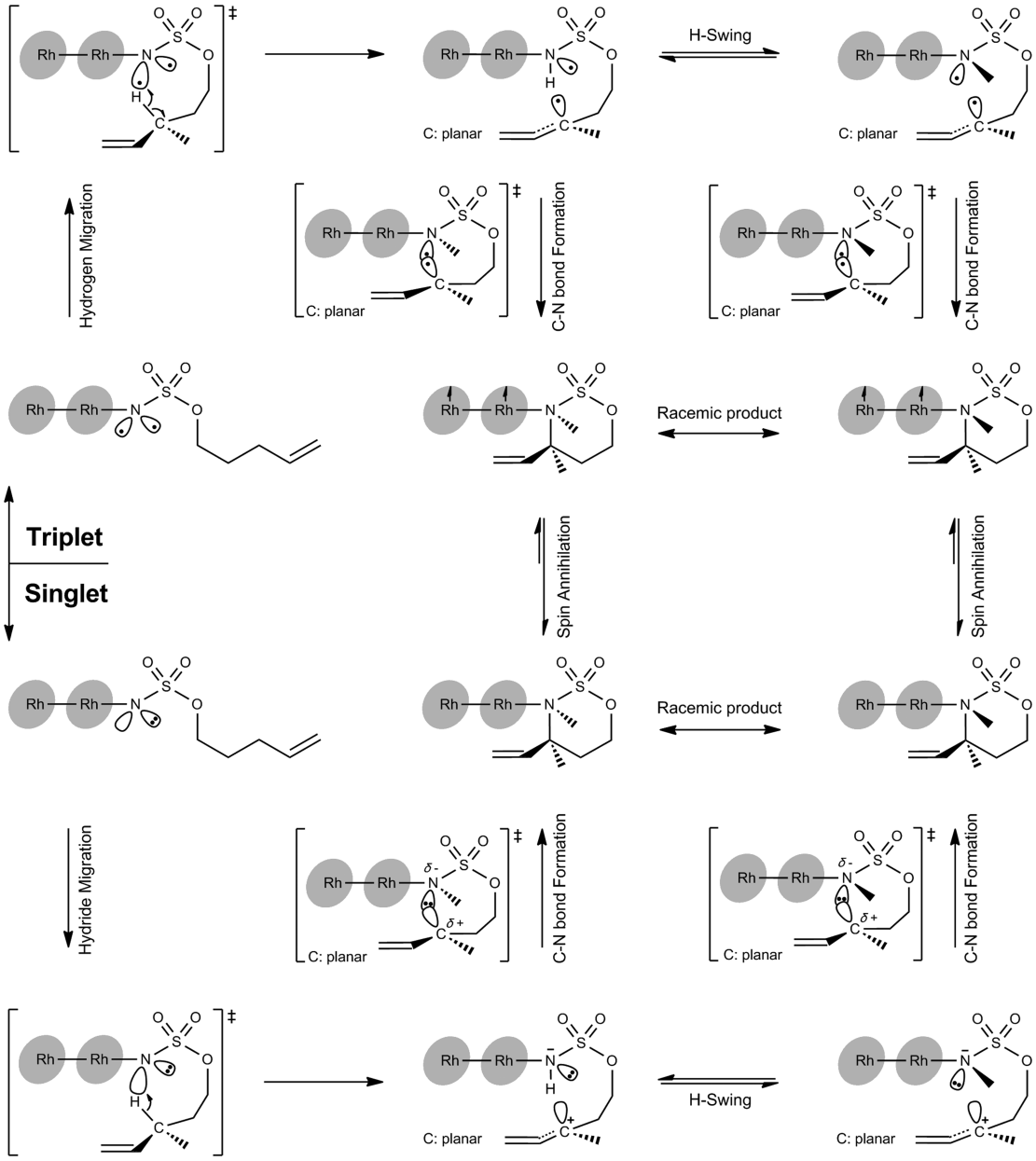

Scheme 2. Universal Reaction Mechanisms of the Dirhodium Catalyzed Alkene Aziridination Reactions

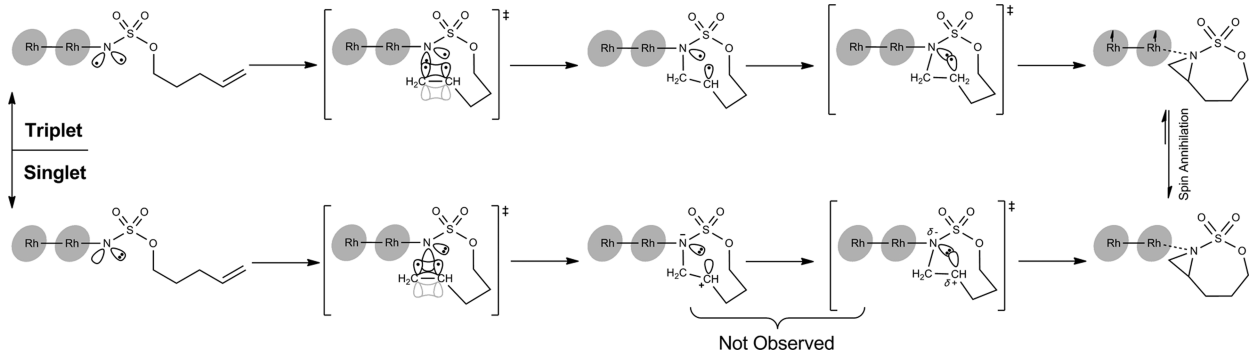

sufficient N center in the singlet intermediate. The subsequent combination of the positive allylic carbocation and the negative N center is observed in the product-determining steps. However, the singlet stepwise pathway is not obtained in the alkene aziridination reactions. This is estimated to be due to the poor stabilization of the potential carbocation and the close distance

dx.doi.org/10.1021/jo5019987 | J. Org. Chem. XXXX, XXX, XXX−XXX

between the negative N center and the positive C1 center. Therefore, the nature of C−H amination and alkene aziridination is a stepwise process and strongly donating catalysts are favorable upon observation of the stepwise pathways. A mixed singlet−triplet pathway is preferred in either the C−H insertion or alkene aziridination in the $Rh_2(NCH_3CHO)_4$ entry where the triplet coordinate is initially favorable in the rate-determining steps and the resultant triplet intermediates would convert to a singlet spin state via the MECPs located before the C−N formation steps and then follow the singlet coordinate to obtain the singlet product. Significant spin−orbital coupling is observed in the dirhodium center in this kind of MECP. The $Cl-Rh_2(OAc)_4$ entry is utilized to explore the electronic effect from the group coordinated to the other axial site of the dirhodium paddlewheel complexes. The added chloride acts as an electron-donor group due to the significant Cl p_x/p_y and Rh−Rh $d_{xz}-d_{xz}/d_{yz}-d_{yz}$ orbital interactions.

The electronic effect on the chemoselectivity is majorly explored, and the results show that triplet reactants are relatively more stable than their singlet counterparts and strongly donating groups would further stabilize the triplet species and subsequently prefer a triplet coordinate. Meanwhile, strongly donating groups are favorable in C−H amination reactions while the alkene aziridination reactions are predominant in the poor electron-donor systems.

To conclude, our theoretical efforts are consistent with the experimental observations and, more importantly, provide a thorough understanding of the nature of intramolecular C−H amination and alkene aziridination reaction pathways. The theoretical approach presented in the paper will contribute to the rational design of future catalysts.

■ ASSOCIATED CONTENT

Supporting Information

Figures S1, S2, and S3 of optimized structures. Figure S4 of the mode A, B, C, and E related alkene aziridination mechanisms. Figure S5 of IRC calculations performed on 1-$^1TS_{A\text{-}G}$. Figure S6 of the proposed I-A and I-B C−H amination pathways in the $Rh_2(OAc)_4$ entry. Table S1 of the NBO charge of the $Rh_2(NCH_3CHO)_4$ promoted reactions. Figure S7 of the comparison of I-B1 and I-B2 pathways in the $Rh_2(NCH_3CHO)_4$ entry. This material is available free of charge via the Internet at http://pubs.acs.org.

■ AUTHOR INFORMATION

Corresponding Author

*E-mail: ceszhcy@mail.sysu.edu.cn.

Notes

The authors declare no competing financial interest.

■ ACKNOWLEDGMENTS

We gratefully acknowledge the National Natural Science Foundation of China (Grant Nos. 20973204, 21173273, and 21373277) for financial support. The research is also partially supported by the high performance grid computing platform of Sun Yat-Sen University, the Guangdong Province Key Laboratory of Computational Science, and the Guangdong Province Computational Science Innovative Research Team.

■ REFERENCES

(1) (a) Müller, P.; Fruit, C. *Chem. Rev.* **2003**, *103*, 2905. (b) Davies, H. M. L.; Long, M. S. *Angew. Chem., Int. Ed.* **2005**, *44*, 3518. (c) Davies, H. M. L. *Angew. Chem., Int. Ed.* **2006**, *45*, 6422. (d) Doyle, M. P. *J. Org. Chem.* **2006**, *71*, 9253. (e) Davies, H. M. L.; Manning, J. R. *Nature* **2008**, *451*, 417. (f) Díaz-Requejo, M. M.; Pérez, P. J. *Chem. Rev.* **2008**, *108*, 3379. (g) Hansen, J.; Davies, H. M. L. *Coord. Chem. Rev.* **2008**, *252*, 545. (h) Collet, F.; Dodd, R. H.; Dauban, P. *Chem. Commun.* **2009**, 5061. (i) Roizen, J. L.; Harvey, M. E.; Du Bois, J. *Acc. Chem. Res.* **2012**, *45*, 911. (j) Yamaguchi, J.; Yamaguchi, A. D.; Itami, K. *Angew. Chem., Int. Ed.* **2012**, *51*, 8960.

(2) (a) Breslow, R.; Gellman, S. H. *J. Am. Chem. Soc.* **1983**, *105*, 6728. (b) Au, S.-M.; Huang, J.-S.; Yu, W.-Y.; Fung, W.-H.; Che, C.-M. *J. Am. Chem. Soc.* **1999**, *121*, 9120. (c) Liang, J.-L.; Yuan, S.-X.; Huang, J.-S.; Yu, W.-Y.; Che, C.-M. *Angew. Chem., Int. Ed.* **2002**, *41*, 3465. (d) Liang, J.-L.; Yuan, S.-X.; Huang, J.-S.; Che, C.-M. *J. Org. Chem.* **2004**, *69*, 3610. (e) Yu, X.-Q.; Huang, J.-S.; Zhou, X.-G.; Che, C.-M. *Org. Lett.* **2000**, *2*, 2233. (f) Paradine, S. M.; White, M. C. *J. Am. Chem. Soc.* **2012**, *134*, 2036. (g) Zhou, X.-G.; Yu, X.-Q.; Huang, J.-S.; Che, C.-M. *Chem. Commun.* **1999**, 2377.

(3) (a) Yamawaki, M.; Tsutsui, H.; Kitagaki, S.; Anada, M.; Hashimoto, S. *Tetrahedron Lett.* **2002**, *43*, 9561. (b) Liang, J.-L.; Yuan, S.-X.; Chan, P. W. H.; Che, C.-M. *Tetrahedron Lett.* **2003**, *44*, 5917. (c) Catino, A. J.; Forslund, R. E.; Doyle, M. P. *J. Am. Chem. Soc.* **2004**, *126*, 13622. (d) Fruit, C.; Müller, P. *Helv. Chim. Acta* **2004**, *87*, 1607. (e) Catino, A. J.; Nichols, J. M.; Forslund, R. E.; Doyle, M. P. *Org. Lett.* **2005**, *7*, 2787. (f) Lebel, H.; Huard, K.; Lectard, S. *J. Am. Chem. Soc.* **2005**, *127*, 14198. (g) Guthikonda, K.; Wehn, P. M.; Caliando, B. J.; Du Bois, J. *Tetrahedron* **2006**, *62*, 11331. (h) Liang, C.; Robert-Peillard, F.; Fruit, C.; Müller, P.; Dodd, R. H.; Dauban, P. *Angew. Chem., Int. Ed.* **2006**, *45*, 4641. (i) Reddy, R. P.; Davies, H. M. L. *Org. Lett.* **2006**, *8*, 5013. (j) Fiori, K. W.; Du Bois, J. *J. Am. Chem. Soc.* **2007**, *129*, 562. (k) Liang, C.; Collet, F.; Robert-Peillard, F.; Müller, P.; Dodd, R. H.; Dauban, P. *J. Am. Chem. Soc.* **2007**, *130*, 343. (l) Zalatan, D. N.; Du Bois, J. *J. Am. Chem. Soc.* **2008**, *130*, 9220. (m) Fiori, K. W.; Espino, C. G.; Brodsky, B. H.; Du Bois, J. *Tetrahedron* **2009**, *65*, 3042. (n) Bess, E. N.; DeLuca, R. J.; Tindall, D. J.; Oderinde, M. S.; Roizen, J. L.; Du Bois, J.; Sigman, M. S. *J. Am. Chem. Soc.* **2014**, *136*, 5783. (o) Harvey, M. E.; Musaev, D. G.; Du Bois, J. *J. Am. Chem. Soc.* **2011**, *133*, 17207. (p) Nägeli, I.; Baud, C.; Bernardinelli, G.; Jacquier, Y.; Moraon, M.; Müllet, P. *Helv. Chim. Acta* **1997**, *80*, 1087.

(4) (a) Zhang, J.; Hong Chan, P. W.; Che, C.-M. *Tetrahedron Lett.* **2005**, *46*, 5403. (b) Badiei, Y. M.; Krishnaswamy, A.; Melzer, M. M.; Warren, T. H. *J. Am. Chem. Soc.* **2006**, *128*, 15056. (c) Milczek, E.; Boudet, N.; Blakey, S. *Angew. Chem., Int. Ed.* **2008**, *47*, 6825. (d) Ohta, C.; Katsuki, T. *Tetrahedron Lett.* **2001**, *42*, 3885. (e) Müller, P.; Boléa, C. *Helv. Chim. Acta* **2002**, *85*, 483.

(5) Lin, X.; Zhao, C.; Che, C.-M.; Ke, Z.; Phillips, D. L. *Chem.—Asian J.* **2007**, *2*, 1101.

(6) (a) Davies, H. M. L.; Beckwith, R. E. J. *Chem. Rev.* **2003**, *103*, 2861. (b) Nakamura, E.; Yoshikai, N.; Yamanaka, M. *J. Am. Chem. Soc.* **2002**, *124*, 7181. (c) Nowlan, D. T.; Gregg, T. M.; Davies, H. M. L.; Singleton, D. A. *J. Am. Chem. Soc.* **2003**, *125*, 15902. (d) Wong, F. M.; Wang, J.; Hengge, A. C.; Wu, W. *Org. Lett.* **2007**, *9*, 1663. (e) Barman, D. N.; Liu, P.; Houk, K. N.; Nicholas, K. M. *Organometallics* **2010**, *29*, 3404. (f) Lin, X.; Xi, Y.; Sun, J. *Comput. Theor. Chem.* **2012**, *999*, 74. (g) Guo, Z.; Guan, X.; Huang, J.-S.; Tsui, W.-M.; Lin, Z.; Che, C.-M. *Chem.—Eur. J.* **2013**, *19*, 11320. (h) Zhang, X.; Ke, Z.; DeYonker, N. J.; Xu, H.; Li, Z.-F.; Xu, X.; Zhang, X.; Su, C.-Y.; Phillips, D. L.; Zhao, C. *J. Org. Chem.* **2013**, *78*, 12460.

(7) (a) Hansch, C.; Leo, A.; Taft, R. W. *Chem. Rev.* **1991**, *91*, 165. (b) Wang, J.; Chen, B.; Bao, J. *J. Org. Chem.* **1998**, *63*, 1853.

(8) Davies, H. M. L.; Hansen, T.; Churchill, M. R. *J. Am. Chem. Soc.* **2000**, *122*, 3063.

(9) (a) Newcomb, M.; Toy, P. H. *Acc. Chem. Res.* **2000**, *33*, 449. (b) Choi, S.-Y.; Toy, P. H.; Newcomb, M. *J. Org. Chem.* **1998**, *63*, 8609.

(10) Collet, F.; Lescot, C.; Liang, C.; Dauban, P. *Dalton Trans.* **2010**, *39*, 10401.

(11) (a) Nguyen, Q.; Sun, K.; Driver, T. G. *J. Am. Chem. Soc.* **2012**, *134*, 7262. (b) Lorpitthaya, R.; Xie, Z.-Z.; Sophy, K. B.; Kuo, J.-L.; Liu, X.-W. *Chem.—Eur. J.* **2010**, *16*, 588. (c) Lorpitthaya, R.; Xie, Z.-Z.; Kuo, J.-L.; Liu, X.-W. *Chem.—Eur. J.* **2008**, *14*, 1561.

dx.doi.org/10.1021/jo5019987 | *J. Org. Chem.* XXXX, XXX, XXX−XXX

(12) Aguila, M. J. B.; Badiei, Y. M.; Warren, T. H. *J. Am. Chem. Soc.* **2013**, *135*, 9399.
(13) (a) Liu, Y.; Guan, X.; Wong, E. L.-M.; Liu, P.; Huang, J.-S.; Che, C.-M. *J. Am. Chem. Soc.* **2013**, *135*, 7194. (b) Lyaskovskyy, V.; Suarez, A. I. O.; Lu, H.; Jiang, H.; Zhang, X. P.; de Bruin, B. *J. Am. Chem. Soc.* **2011**, *133*, 12264.
(14) Espino, C. G.; Du Bois, J. *Angew. Chem., Int. Ed.* **2001**, *40*, 598.
(15) Maestre, L.; Sameera, W. M. C.; Díaz-Requejo, M. M.; Maseras, F.; Pérez, P. J. *J. Am. Chem. Soc.* **2012**, *135*, 1338.
(16) Han, H.; Park, S. B.; Kim, S. K.; Chang, S. *J. Org. Chem.* **2008**, *73*, 2862.
(17) Bodner, R.; Marcellino, B. K.; Severino, A.; Smenton, A. L.; Rojas, C. M. *J. Org. Chem.* **2005**, *70*, 3988.
(18) Cundari, T. R.; Jimenez-Halla, J. O. C.; Morello, G. R.; Vaddadi, S. *J. Am. Chem. Soc.* **2008**, *130*, 13051.
(19) (a) Wehn, P. M.; Du Bois, J. *Org. Lett.* **2005**, *7*, 4685. (b) Fruit, C.; Müller, P. *Tetrahedron: Asymmetry* **2004**, *15*, 1019.
(20) Harvey, J. N.; Aschi, M.; Schwarz, H.; Koch, W. *Theor. Chem. Acc.* **1998**, *99*, 95.
(21) Frisch, M. J.; Trucks, G. W.; Schlegel, H. B.; Scuseria, G. E.; Robb, M. A.; Cheeseman, J. R.; Scalmani, G.; Barone, V.; Mennucci, B.; Petersson, G. A.; Nakatsuji, H.; Caricato, M.; Li, X.; Hratchian, H. P.; Izmaylov, A. F.; Bloino, J.; Zheng, G.; Sonnenberg, J. L.; Hada, M.; Ehara, M.; Toyota, K.; Fukuda, R.; Hasegawa, J.; Ishida, M.; Nakajima, T.; Honda, Y.; Kitao, O.; Nakai, H.; Vreven, T.; Montgomery, J. A., Jr.; Peralta, J. E.; Ogliaro, F.; Bearpark, M.; Heyd, J. J.; Brothers, E.; Kudin, K. N.; Staroverov, V. N.; Kobayashi, R.; Normand, J.; Raghavachari, K.; Rendell, A.; Burant, J. C.; Iyengar, S. S.; Tomasi, J.; Cossi, M.; Rega, N.; Millam, J. M.; Klene, M.; Knox, J. E.; Cross, J. B.; Bakken, V.; Adamo, C.; Jaramillo, J.; Gomperts, R.; Stratmann, R. E.; Yazyev, O.; Austin, A. J.; Cammi, R.; Pomelli, C.; Ochterski, J. W.; Martin, R. L.; Morokuma, K.; Zakrzewski, V. G.; Voth, G. A.; Salvador, P.; Dannenberg, J. J.; Dapprich, S.; Daniels, A. D.; Farkas, O.; Foresman, J. B.; Ortiz, J. V.; Cioslowski, J.; Fox, D. J. In *Gaussian 09*, Revision A.01; Gaussian, Inc.: Wallingford, CT, 2009.
(22) (a) Becke, A. D. *J. Chem. Phys.* **1993**, *98*, 1372. (b) Perdew, J. P.; Burke, K.; Wang, Y. *Phys. Rev. B* **1996**, *54*, 16533.
(23) Zhao, Y.; Truhlar, D. G. *J. Chem. Phys.* **2006**, *125*, 194101.
(24) Lin, X.; Che, C.-M.; Phillips, D. L. *J. Org. Chem.* **2007**, *73*, 529.
(25) (a) Huang, G.; Xie, K.; Lee, D.; Xia, Y. *Org. Lett.* **2012**, *14*, 3850. (b) Xu, H.; Zhang, X.; Ke, Z.-F.; Li, Z.-F.; Xu, X.-Y.; Su, C.-Y.; Phillips, D. L.; Zhao, C. *RSC Adv.* **2013**, *3*, 17131.
(26) (a) Steinbrenner, U.; Bergner, A.; Dolg, M.; Stoll, H. *Mol. Phys.* **1994**, *82*, 3. (b) Henglein, A. *J. Phys. Chem.* **1993**, *97*, 5457.
(27) Lam, W. H.; Lam, K. C.; Lin, Z.; Shimada, S.; Perutz, R. N.; Marder, T. B. *Dalton Trans.* **2004**, 1556.
(28) Hansen, J.; Autschbach, J.; Davies, H. M. L. *J. Org. Chem.* **2009**, *74*, 6555.
(29) Fukui, K. *Acc. Chem. Res.* **1981**, *14*, 363.
(30) Marenich, A. V.; Cramer, C. J.; Truhlar, D. G. *J. Phys. Chem. B* **2009**, *113*, 6378.
(31) Reed, A. E.; Curtiss, L. A.; Weinhold, F. *Chem. Rev.* **1988**, *88*, 899.

dx.doi.org/10.1021/jo5019987 | *J. Org. Chem.* XXXX, XXX, XXX−XXX